Materials Science and Engineering A 528 (2011) 1558–1566

Contents lists available at ScienceDirect

Materials Science and Engineering A

journal homepage: www.elsevier.com/locate/msea

The kinetics and energetics of dislocation mediated de-twinning in nano-twinned face-centered cubic metals

Yujie Wei*

State Key Laboratory of Nonlinear Mechanics, Institute of Mechanics, Chinese Academy of Sciences, Bei Si Huan Xi Road #15, Beijing 100190, PR China

ARTICLE INFO

Article history:
Received 23 September 2010
Received in revised form 20 October 2010
Accepted 25 October 2010

Keywords:
De-twinning
Twinning
Nano-twinned polycrystalline
Strength softening

ABSTRACT

Polycrystalline Cu with hierarchy microstructures – ultrafined grains about 500 nm and included twins several to tens of nanometers thick – show maximum strength at an averaged twin thickness of 15 nm. Li et al. Nature 464 (2010) 877–880 (Ref. [1]), reported that the primary plastic deformation transits from inclined dislocation gliding to de-twinning in nano-twinned (nt) Cu when twin thicknesses decrease from 25 nm to 4 nm. Their investigation showed that enhanced de-twinning accounts for the strength softening in nt-Cu. From the kinetic and energetic aspects of de-twining process, we present respectively two models. In the kinetic model, we assume that thermally activated dislocation nucleation is the controlling mechanism for plastic deformation, while the transformation energy associated with de-twinning is considered to be governing in the energetic model. Applications of the models on strain-rate sensitivity and temperature dependence of strengths in nt-Cu suggest that the energetic mechanism also plays an important role for de-twinning in nt-Cu.

© 2010 Elsevier B.V. All rights reserved.

1. Introduction

With increasing volume fraction of grain boundaries (GBs) as grain sizes reduce, nanocrystalline (nc) metals often exhibit substantial increasing in strength [2–4], but poor deformability, low thermal conductivity, and high electrical resistance [4–6]. Manipulating the GB structures in nc metals such that desired properties can be realized, which is often called GB engineering [4,6–10], has been one of the foci for material synthesis in recent years. The ways to replace general GBs by low energy, coherent twin boundaries (TBs) have been broadly explored [5,11–16], for the well known strengthening mechanism by TBs yet their minimum impairment to mechanical, thermal and electrical properties of polycrystalline metals. A hierarchy structure in polycrystalline Cu, with ultrafine grains and included twins at tens of nanometers thick, has been revealed to be an optimal microstructure [5]. In contrast to conventional coarse-grained Cu, such nt-Cu shows high strength, intermediate ductility, and almost no loss in electrical conductivity [5]. Comprehensive summary on the progress in this field is documented in [6] and [17].

More interestingly, Lu et al. [18] have revealed that, in samples with similar grain sizes but different twin thicknesses, the strength of nt-Cu first increases as twin thickness λ decreases to 15 nm, then decreases as λ gets even smaller (see Fig. 1). The strength softening with further decreasing of λ from 15 nm to 4 nm is particularly intriguing. In nc metals without embedded twins, there is a strength softening as grain sizes reach about 10 nm and smaller. Such softening is generally related to the shift of major plastic deformation mechanisms – from dislocation mediated plastic deformation to GB associated mechanisms such as GB sliding, GB diffusion and grain rotation [7–9] when grains become smaller than 10 nm, which are intensively investigated by experiments [7,19–21], molecular dynamics (MD) simulations [22–27], and continuum level models [28–34]. Nevertheless, the experience for strength softening in regular nc metals cannot be applied to nt-Cu. In nt-Cu, plastic deformation mainly comes from three sources: (I) GB associated deformation, (II) motion and/or nucleation of dislocations inclined to TBs, and (III) nucleation, motion and/or multiplication of dislocations parallel to TBs (see Fig. 2 for demonstration). For case (I), it is known from experiments that the grain sizes for those samples with different twin thicknesses are close, and the contribution by GB deformation, if it exists, should be similar in all samples. Indeed, the enhanced ductility in nt-Cu may suggest that plastic deformation in GBs is very small, since we know that non-creep deformation in GBs usually leads to poor ductility in polycrystalline materials. As to case (II), nucleation and motion of dislocations inclined to TBs account for the strengthening mechanism as λ decreases instead of softening. Because dislocation activities are confined by the twin space λ, it renders the difficulty in the motion and nucleation of such inclined dislocations. Therefore, to shed light on the observed strength softening in nt-Cu as λ gets smaller, it is necessary to investigate case (III) – the nucleation, motion, and/or multiplication of

* Fax: +86 10 82543977.
E-mail address: yujie_wei@lnm.imech.ac.cn

0921-5093/$ – see front matter © 2010 Elsevier B.V. All rights reserved.
doi:10.1016/j.msea.2010.10.072

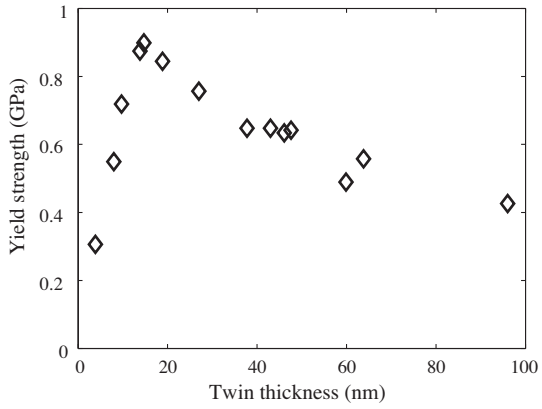

Fig. 1. The yield strength vs. twin thickness in nano-twinned Cu samples with the same average grain size about 500 nm.
Data replotted from [18].

dislocations parallel to TBs. The motion of leading partial dislocations in TBs will result in de-twinning, also called TB migration in f.c.c. metals, since the gliding of a leading partial dislocation in the TB renders the TB behind the dislocation to migrate by one (1 1 1) lattice space. For now and in what follows, we refer leading partial dislocations in TBs as twinning partials.

Deformation mechanisms in such nano-twinned metals have been studied by experiments [35–41], MD simulations [42–50], and finite-element simulations [51,52]. However, the softening mechanism in nt-Cu has not been studied in depth. The initial dislocation density observed in nt-Cu [18] could contribute roughly 0.2% plastic strain if all initial dislocations are mobile. After the exhaustion of those initial dislocations, the flow stress in samples with narrower twins is still much lower than those with wider twins in a wide strain range, say from 2% to 10% strain in the stress–strain curve (Ref. [18], their Fig. 3). It hence indicates that, in addition to the influence by initial dislocations, there might be other mechanisms responsible for the strength softening of nt-Cu. MD simulations by Kulkarni and Asaro [53] showed that pre-existing dislocations influence the initial strength of nt-metals. They also speculated that the influence of twin–twin interactions may contribute to strength softening. Large scale MD simulations by Li et al. [1] show that there exists a transition of dislocation activities: from nucleation of

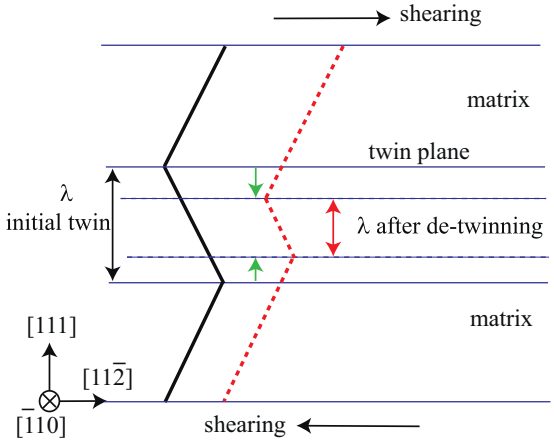

Fig. 2. Diagrams to show the de-twinning process via emission of twinning partials. The initial twin gets thinner in response to the applied shearing. The moving twin planes from solid blue lines to dotted blues result from emission of twinning partials in successive layers. Note that the role of twins and matrices can be switched if we change the shearing direction (For interpretation of references to color in this figure legend, the reader is referred to the web version of this article).

inclined dislocations (with respect to TBs) to nucleation of twinning partials as twin thickness narrows; the refinement of twin structure at a fixed grain size increases the density of nucleation sites for twinning partials and therefore softens the material by easy nucleation mechanism. Here we will show that, in addition to the kinetics of twinning partial nucleation controlled de-twining, the energetics of de-twinning also plays an important role for strength softening in nt-Cu in order to explain the strain-rate sensitivity and temperature dependence of this material. The energetic mechanism predicts that the strength τ is proportional to twin thickness λ and inversely proportional to grain size d, i.e., $\tau \propto \lambda/d$.

The remainder of this paper is organized as follows. In Section 2, we briefly discuss the MD simulations by Li et al. [1] to motivate our subsequent discussion. In Section 3, we then describe modeling on twinning partial mediated de-twinning. Two situations are considered separately: one is the nucleation of twinning partials being the controlling mechanism; the other corresponds to easy twinning partial sources (either nucleated, pre-existing, or by multiplication) but their successful motion to accommodate plastic deformation is controlled by free energy change during de-twinning. Both mechanisms lead to strength softening in nt-Cu as TB thickness decreases. Two characteristics of those mechanisms – strain-rate sensitivity and temperature dependence – are discussed in Section 4. We conclude in Section 5 with some suggestions on further experiments which might better our understanding on the deformation of nt-metals.

2. Mechanisms revealed by atomic simulations in nt-Cu by Li et al. [1]

Li et al. [1] have performed large-scale MD simulations of plastic deformation mechanisms in two- and three-dimensional polycrystalline nano-twinned samples with grain sizes ranging from 10 to 70 nm and twin thicknesses ranging from 0.83 to 25 nm. Their simulations using embedded atomic potential [54–57] show that there exists a transition in deformation mechanism in initially dislocation-free nt-Cu samples, from dislocations nucleated from GBs but inclined to twin planes to nucleation and motion of twinning partials. A model case of their quasi three-dimensional simulations [1] are shown in Fig. 4. Undeformed samples with $\lambda = 2$ nm and 20 nm are shown in Fig. 4a and b respectively. Fig. 4c and d shows respectively the deformed samples at 15% tensile strain. De-twinning is found to be the dominant plastic deformation mechanism when $\lambda = 2$ nm (Fig. 4c); while $\lambda = 20$ nm, both inclined partial dislocations and twinning partials are broadly observed (Fig. 4d). For a better view about the transition of dislocation activities in 3D samples, the reader is referred to [1]. We present next two models on twinning partial mediated de-twinning.

3. Modeling on strength controlled by dislocation mediated de-twinning

Twinning/de-twinning in f.c.c. metals is believed to result from the emission of twinning partials on successive atomic layers in {1 1 1} planes, and such twinning partials could be nucleated from GBs or be multiplied by dislocation–twin boundary interaction [58]. A broadly used criterion for the activation of complete dislocations vs. twinning partials is based on the competition of intrinsic stacking energy over unstable stacking fault energy [59]. Such a criterion, however, does not account for directionality in twinning [60,61]. It is known that twinning occurs in only one $< 11\bar{2} >$ -type direction in a {1 1 1} plane since twinning mode should lead to the smallest possible shearing [60]. The "inverse grain-size effect" on twinning – higher chance of deformation twinning in bigger grains in nc Ni samples after deformation [62] – cannot be explained by the stack-

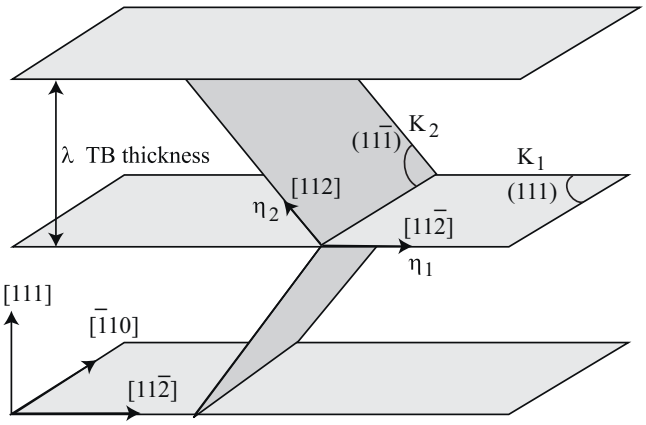

Fig. 3. One twin–matrix pair with crystallographic directions and twin elements $\{K_1, \eta_1, K_2, \eta_2\}$ for shear strain $e^T = 0.707$.

ing fault energy based criterion. Effective twinning/de-twinning is generally conditioned on two things: (a) sufficiently high local stress to trigger nucleation of twinning partials on successive layers, and (b) energetically favored transformation. In the following subsections, we will supply theoretical explanations for nucleation and energy controlled de-twinning, respectively. We note that the kinetics and energetic of de-twinning are not necessary two different viewpoints on plasticity by de-twinning, but rather refer to the nucleation and growth aspects of the de-twinning process. It is desired to combine these two stages of deformation in a single model since nucleation and growth are naturally coupled processes in de-twinning. However, such a unified treatment faces the challenges of (a) dealing with rate-dependent and rate-independent plasticity in the same scheme, and (b) developing non-local plastic deformation by twinning partials. Numerical tools are needed to address those coupled processes, which is not included in this paper.

3.1. Kinetics controlled twinning/de-twinning

A kinetic model for twinning partial nucleation controlled strength softening has been given in [1]. We adopt the model here with slight modifications. The motive to treat de-twinning in nt-Cu as a rate controlled mechanism is that it is accommodated by twinning partials nucleated from the intersections of GBs and twin planes [1,36–39]. Considering a twinning partial on the slip system α swept across the grain, the plastic strain increment $\Delta\gamma^{(\alpha)}$ in a twin–matrix pair (Fig. 3) by such an emission is [1]

$$\Delta\gamma^{(\alpha)} = \frac{b}{2\lambda}\left(\mathbf{b}^{(\alpha)} \otimes \mathbf{m}^{(\alpha)} + \mathbf{m}^{(\alpha)} \otimes \mathbf{b}^{(\alpha)}\right) \tag{1}$$

where b is the magnitude of the Burgers vector of a twinning partial, and $\mathbf{b}^{(\alpha)}$ and $\mathbf{m}^{(\alpha)}$ are the Burgers vector and the plane normal of the αth slip system, respectively. Both are unit vectors. For simplicity, we rewrite Eq. (1) in scalar format and convert it to macroscopic strain incremental $\Delta\varepsilon$

$$\Delta\varepsilon = \beta\frac{b}{2\lambda} \tag{2}$$

where β is a coefficient combined the effect from all active de-twinning systems and the texture effect. The macroscopic strain rate given by such an twinning partial is given as [63,64].

$$\dot{\varepsilon} = \frac{\Delta\varepsilon}{\Delta t} = \beta\frac{b}{2\lambda}\upsilon_s \tag{3}$$

where Δt is the total time needed for a successful emission and υ_s is the successful jumping frequency. Δt includes both traveling time and incubation time, and the former is usually much shorter than the latter. Hence we can estimate Δt based on thermal vibration of atoms in the junction of a TB and a GB. Unlike the gliding of complete dislocations, twinning partials can only move in one direction along a slip system, hence

$$\upsilon_s = n\upsilon_t \exp\left(\frac{-\tau_0 V^*}{kT}\right)\exp\left(\frac{\tau}{\phi}\frac{V^*}{kT}\right) \tag{4}$$

where n is the number of potential sites, υ_t is the attempt frequencies of an atomic cluster with activation volume V^*; k and T are the Boltzmann constant and temperature, respectively; τ is the resolved shear stress and τ_0 the threshold shear resistance for the emission of twinning partials; and ϕ is a factor influenced by stress concentration and crystallographic texture. We will take ϕ as a fitting parameter because of the difficulty to determine it precisely[2]. It is noted that both τ_0 and the activation volume V^* are temperature dependent, and the latter may depend on τ as well. In our late discussion, we assume that the changes of τ_0 and V^* as T varies in 290 K–310 K is negligible. Based on finite-element analysis [1], the junctions of GBs and TBs are sites with stress concentration. Hence the potential sites n in one twin–matrix pair is proportional to the atom number in the peripheral of the twin–matrix pair, which is estimated to be

$$n = \frac{\pi d}{b} \tag{5}$$

The attempt frequency υ_t can be related to the Debye frequency υ_d by [65]

$$\nu_t = \nu_d\frac{b}{l} \approx \nu_d\sqrt{\frac{\Omega_0}{V^*}} \tag{6}$$

where l is a characteristic length associated with the activation volume, and is approximated to[3] $l \approx \sqrt{V^*/b}$, and Ω_0 is the atomic volume. Substituting Eqs. (4)–(6) into Eq. (3), we have

$$\dot{\varepsilon} = \nu_D\frac{\beta\pi}{2}\frac{d}{\lambda}\sqrt{\frac{\Omega_0}{V^*}}\exp\left(\frac{-\tau_0 V^*}{kT}\right)\exp\left(\frac{\tau V^*}{\phi kT}\right) \tag{7}$$

At low stress level ($\tau V^*/\phi \ll kT$), the nucleation of twinning partials will give rise to a creep rate proportional to stress. Inverting Eq. (7) and we obtain the stress in terms of strain rate.

$$\frac{\tau}{\phi} = \tau_0 - \frac{kT}{V^*}\ln\left(\frac{\beta\pi}{2}\frac{\nu_D}{\dot{\varepsilon}}\frac{d}{\lambda}\sqrt{\frac{\Omega_0}{V^*}}\right) \tag{8}$$

From Eq. (7), we can calculate the strain-rate sensitivity parameter m, where $m = \partial\ln\tau/\partial\ln\dot{\varepsilon}$ can be interpreted as the slope of

[1] It is assumed that a twinning partial, once emitted, can transverse the whole grain, consequentially lead to de-twinning of one layer of atoms, and the free energy change associated with the de-twinning process favors the complete process – from the nucleation of a twinning partial in a GB to its landing in the opposite GB. It differs from the energetic controlled situation, where the energy associated with de-twinning determines whether twinning partials can sweep through the whole grain.

[2] In a sample with random texture and the twelve de-twinning systems being equally operative, $\phi = M/k_t$, where M is two times of the Taylor factor by taking the directionality of de-twinning into account , and k_t is the average stress concentration factor at the junction of GBs and TBs. The strong initial (1 1 1) texture along the deposition plane [5,18], and the limited de-twinning systems (all residing on planes parallel to TBs) imposed by the grain-twin geometry, will result in a greater ϕ, hence it is difficult to quantify ϕ precisely. We estimate that ϕ is on the order of 10.

[3] This approximation is based on the assumption that the activation volume composed of atoms residing in one layer. We note that different approximation to l would not change the softening mechanism by the kinetics controlled de-twinning in nt-Cu.

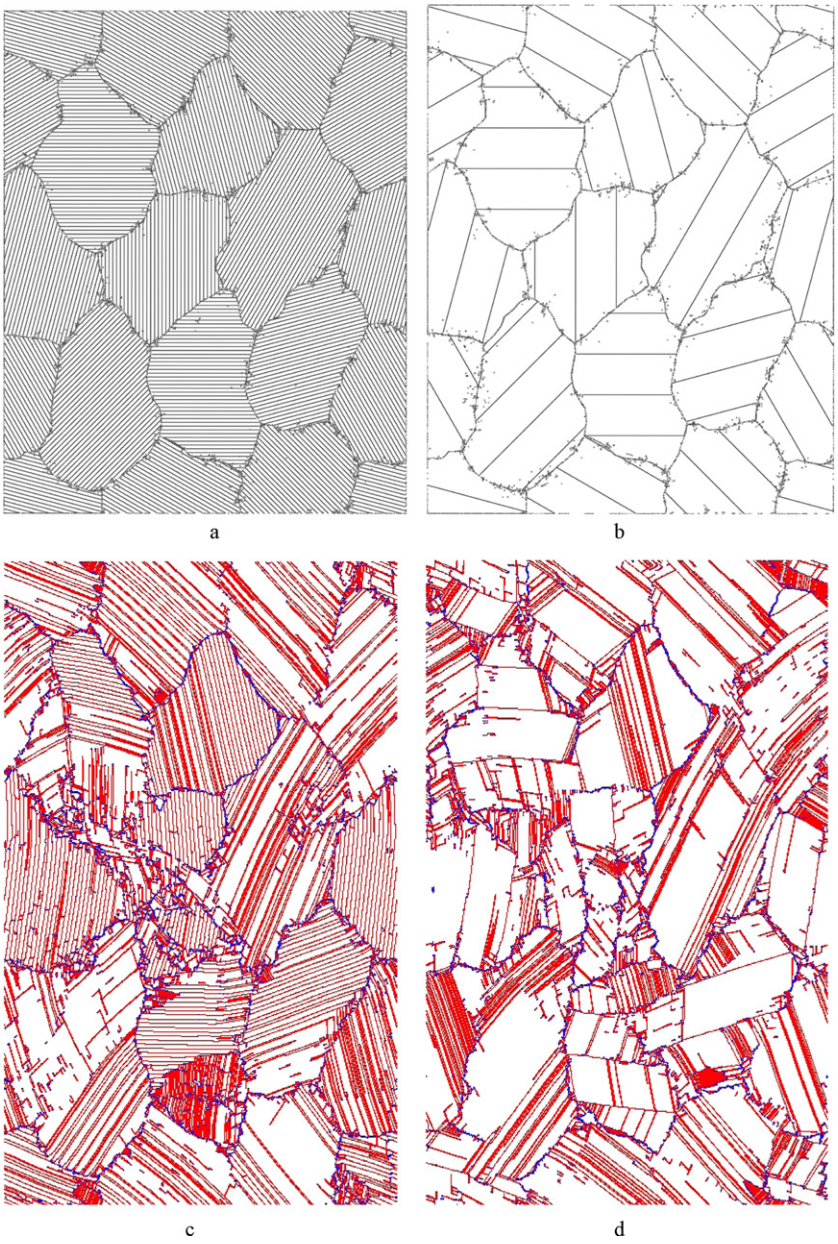

Fig. 4. Atomic simulations on nt-Cu with columnar grains, only non-f.c.c. atoms are shown. The initial structure of twinned polycrystalline Cu with uniform twin thickness (a) λ = 1.88 nm, and (b) λ = 20 nm. The deformation pattern after 15% tensile strain for (c) λ = 1.88 nm and (d) λ = 20 nm.

a graph of $\log(\tau)$ as a function of $\log(\dot{\varepsilon})$. It is convenient to see $m = \phi kT/\tau V^*$, which is the formula given by Conrad [66]. Alternatively, m can be rewritten as

$$\frac{1}{m} = \frac{\tau_0 V^*}{kT} - \ln\left(\frac{\beta\pi}{2}\frac{d}{\lambda}\frac{\nu_D}{\dot{\gamma}}\sqrt{\frac{\Omega_0}{V^*}}\right) \tag{9}$$

We see that m increases as λ decreases – higher strain-rate sensitivity in samples with narrower twins – which qualitatively matches with experimental observations [6,32,67]. Application of the model on twinning partial nucleation controlled twinning/de-twinning will be shown in Section 4.

3.2. Energetics controlled twinning/de-twinning

In previous part, we give the kinetic model for twinning partial nucleation controlled twinning/de-twinning. Here we will only consider situations that either initial twinning partial density is sufficiently high, or the nucleation and/or multiplication of twinning partials are easy. This argument is partly motivated by experimental observations. During electro-deposition, fast deposition rate is required to obtain high density of narrow twins [6,18,68]. Such a process might generate high energy GBs and high density of defects [5,13] when twin thickness is extremely small. Both high density of initial dislocations and high energy GBs may facilitate motion and/or nucleation of twinning partials.

In this circumstance, the free-energy change associated with de-twinning process is controlling. Eshelby's theory [69] is used to derive the free-energy change for shear transformation in an ellipsoid by twinning or de-twinning. Similar idea has been used in the case of martensitic phase transformation [70–72] and precipitate twinning [73]. Since there is no high aspect ratio in those nano-twinned grains [5,18], we assume that de-twinning of thin twins resembles shear transformation of an ellipsoid with semi-axes a, b, and c, with $a = b \approx d$ and $c \approx \lambda$ (see Appendix A for the transformation energy in general ellipsoid with semi-axes $a \geq b \geq c$). Since

$d \gg \lambda$, the elastic energy is given to be [69]:

$$E_{el} = \alpha \frac{\pi}{8} \frac{2-\upsilon}{1-\upsilon} \frac{\lambda}{d} \mu (e^T)^2 V \tag{10}$$

where α is a constant and $V \approx \lambda d^2$, μ is the shear modulus, υ is the Poisson's ratio, and e^T is the shear strain associated with twinning/de-twinning. From Eq. (10), twins are energetically favored to form in a lenticular morphology when V is a constant. A thin disc of thickness approaching zero requires almost no energy for shear transformation e^T. In real crystals, the stacking fault energy induced by such shear transformation restrains the thickness from being extremely small. It is noted that the original Eshelby's theory gives $\alpha = 1$ in Eq. (10) for pure elastic medium. Plastic deformation in the surrounding media, however, may result in lower energy levels. Annealing twins, for example, can grow diffusionally and involve almost no elastic distortion, and hence α approaches to 0, which explains why annealing twins in f.c.c. metals can be several micron thick while deformation twins are in general as thin as tens to several nanometers. Further, only a fraction of λ may be de-twinned. Both situations may result in $0 < \alpha < 1$, as the material undergoes pure elastic deformation and the whole twin is de-twinned, α approaches 1. The change of interaction energy in the presence of a resolved shear stress τ is given as [69]:

$$E_{\text{int}} = -\tau e^T V \tag{11a}$$

and the amount of energy dissipated as twinning partials glide to the opposite end is given as

$$E_{diss} = \tau_l e^T V \tag{11b}$$

where τ_l is the lattice resistance to twinning partials. The interfacial energy change accompanying the transformation is

$$E_{tb} = \psi \gamma_{tb} V / \lambda \tag{12}$$

where γ_{tb} is the energy of a twin-boundary and ψ is a coefficient, $\psi = -2$ for the complete de-twinning of a TB, $\psi = 2$ for the formation of a TB, and $\psi = 0$ for the thickening or thinning of a TB. As initially stress free twinned regions to de-twinning under the applied shear stress τ, the free-energy change per volume is the sum of four contributions: the increasing elastic strain energy in both the de-twinned region and its surrounding media $E_{el,}$ the decreasing elastic energy in the twin as it de-twins E_{int}, the dissipated energy by twinning partial gliding E_{diss}, and the change of interfacial energy by de-twinning E_{tb}. Hence

$$\Delta F = \alpha \frac{\pi}{8} \frac{2-\upsilon}{1-\upsilon} \frac{\lambda}{d} \mu (e^T)^2 - (\tau - \tau_l) e^T + \psi \frac{\gamma_{tb}}{\lambda} \tag{13}$$

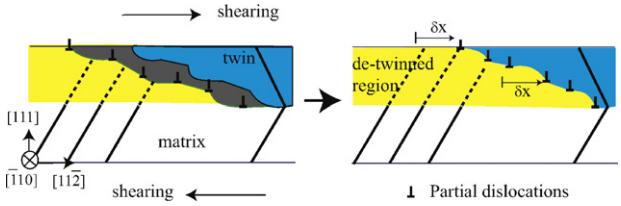

Fig. 5. De-twinning by collective motion of twinning partials (from left to right). Regimes colored in cyan, yellow, and grey stand respectively for original twin, de-twinned part, and to-be de-twinned part. A propagation of δx in the de-twinned zone requires the motion of all twinning partials on successive atomic layers by an amount of δx along [11$\bar{2}$] direction (For interpretation of references to color in this figure legend, the reader is referred to the web version of this article).

For successful twinning or de-twinning, we require $\Delta F \leq 0$ [4]. The critical resolved shear stress to satisfy $\Delta F = 0$ is obtained as

$$\tau = \tau_l + \alpha \frac{\pi}{8} \frac{2-\upsilon}{1-\upsilon} \frac{\lambda}{d} \mu e^T - \frac{2\gamma_{tb}}{\lambda e^T} \tag{14}$$

From Eq. (13) to Eq. (14), we have used $\psi = -2$ to account for reduction of TB energy by complete de-twinning. A dislocation based mechanistic picture [74] is adopted to explain the scaling of $(\tau - \tau_l) \propto \lambda/d$ in Eq. (14). As an applied shear stress extends the de-twinned zone by a distance of δx, it requires the simultaneous (at experimental time scales) advance of δx for twinning partials (Fig. 5). The work done by the shear stress induces the increasing energy by the line extension of all twinning partials follows

$$(\tau - \tau_l) bd\, \delta x = \beta_0 \left(\frac{\lambda}{d_{111}} \right) \mu b^2\, \delta x \tag{15}$$

where β_0 is a factor representing the fraction of de-twinned thickness in the twin with thickness λ, which is in the order of unit, d_{111} is the space between (1 1 1) planes, and λ/d_{111} gives the number of twinning partials. The same scaling of $(\tau - \tau_l) \propto \lambda/d$ shown in Eq. (14) is also seen in Eq. (15).

[4] The interaction energy between two transformations is not considered here. If two transformations occur in the same grain, it is expected that the interaction energy is positive. More energy is needed to transform the second one. The apparent strain-hardening in samples with narrow twins indicates the importance of twin-twin interaction. If the two transformations happen in neighboring grains, the interaction energy is grain-orientation dependent and could be either positive or negative. It seems that the interaction energy is more related to strain hardening than initial yielding. Since our attention is on the size effect of yielding strength in nt Cu, we neglect the influence by interactions between different transformation zones at this moment.

Table 1
Brief description of parameters used for nt-Cu. Parameters obtained by fitting are also indicated.

Description of parameter	Symbol	Value	In equations
Shear modulus at room temperature	μ	45 GPa	Eq. (14)
Poisson's ratio	ν	0.35	Eq. (14)
Testing temperature	T	300 K	Eq. (8)
Applied strain rate	$\dot{\varepsilon}$	6×10^{-3}/s	Eq. (8)
Grain size	d	500 nm	Eqs. (8) and (14)
Twin thickness	λ	4–100 nm	Eqs. (8) and (14)
Geometric factor	β	~1	Eq. (8)
Stress-concentration factor (fitting parameter)	ϕ	4.2	Eq. (8)
Atomic volume	Ω_0	11.8 Å^3	Eq. (8)
Debye frequency	υ_D	1.88×10^{13}/s	Eq. (8)
Threshold shear resistance for emission of leading partial dislocations in TBs	τ_0	$0.01\mu \sim 0.03\mu$	Eq. (8)
Activation volume for dislocation nucleation (fitting parameter)	V^*	$10.6\Omega_0$	Eq. (8)
Transformation strain by twinning/de-twinning	e^T	0.707	Eq. (14)
Shear resistance for twinning partial	τ_l	~10 MPa	Eq. (14)
Twin boundary energy	γ_{tb}	24 mJ/m^2	Eq. (14)
Index parameter	ψ	−2	Eq. (14)
Geometrical factor	α	0.4	Eq. (14)

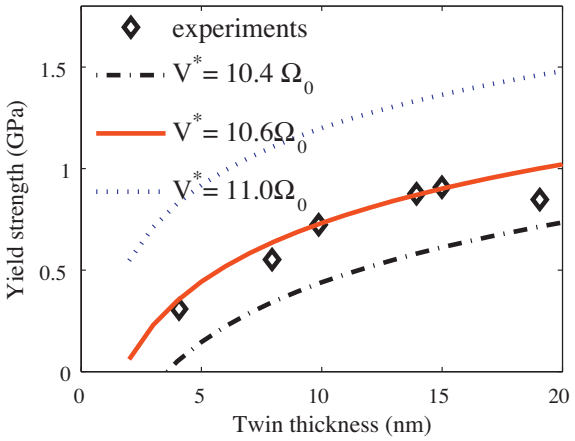

Fig. 6. Yield strength vs. twin thickness from both the model (Eq. (8)) and experiments. Only experimental data (diamond symbols, from Ref. [18]) in the softening region are used. The experimental trend is captured by Eq. (8) using $\phi = 4.2$ and an activation volume $V^* = 10.6\Omega_0$. Two other curves with slightly different activation volume in. Eq. (8) indicate that the predicted shear strength is very sensitive to the activation volume.

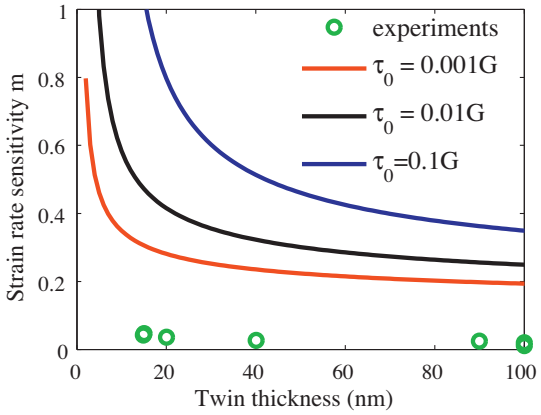

Fig. 7. The strain-rate sensitivity vs. twin thickness for several τ_0. Both the experimental data (from Ref. [6]) and predictions by the kinetic model are shown. Even for a threshold stress $\tau_0 = 0.001\mu$, the predicted strain-rate sensitivity is much higher than the experimental observation.

4. Application of the models to experiments

We will apply the two models given above to experimental data for nt-Cu in this section. Eqs. (8) and (14) will be used to capture the softening part in the strength vs. twin thickness curve shown in Fig. 1. Parameters used for the models are shown in Table 1. Detailed explanation on the choice/derivation of those numbers is given in the main text at appropriate places.

4.1. The kinetics model for de-twinning

In the condition that nucleation of twinning partials is the controlling mechanism for twinning/de-twinning, we need several constant and material parameters in Eq. (8) to determine the critical resolved shear stress, including Boltzmann constant $\{k\}$, parameters for testing conditions $\{T, \dot{\varepsilon}\}$, geometrical parameters and factors $\{d, \lambda, \beta, \phi\}$, and material parameters $\{\Omega_0, \upsilon_D, \tau_0, V^*\}$. The experiments were performed at room temperature, $T = 300$ K, and at a strain rate of $\dot{\varepsilon} = 6 \times 10^{-3}$/s. It is also known that d is about 500 nm [5,18]. For simplicity, we take $\beta = 1$, and ϕ will be used as a fitting parameter. Atomic volume Ω_0 for Cu is about 11.8 Å^3. The

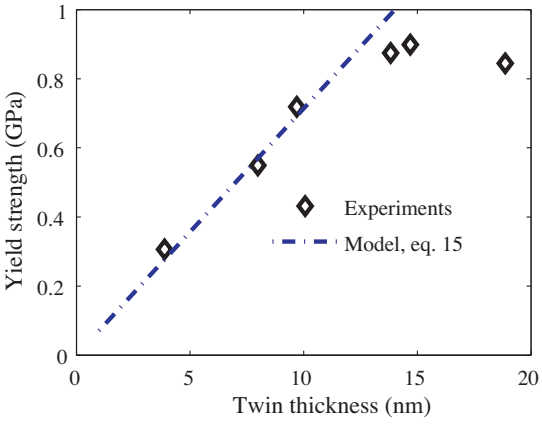

Fig. 8. The tensile strength vs. twin thickness from the model (Eq. (14)) and experiments (Ref. [18]).

Debye frequency υ_D for Cu is given as

$$\nu_D = \left(\frac{3N}{4\pi V}\right)^{1/3} \nu_s$$

Here N/V is the number density of Cu, and ν_s is the sound speed in Cu, which is about 4760 m/s. The critical shear resistance τ_0 for the

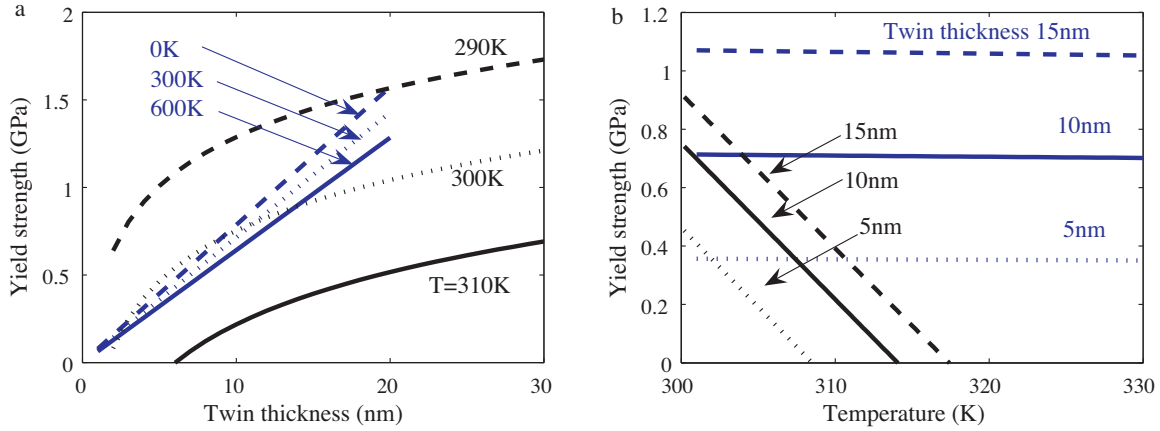

Fig. 9. Temperature dependence of strength in nt-Cu predicted by the kinetic model and the energetic model. Here black curves are for the kinetic model (Eq. (8)) and blue curves are for the energetic model (Eq. (14)): (a) strength vs. twin thickness at several temperatures, and (b) strength vs. temperature for samples with different twin thicknesses (For interpretation of references to color in this figure legend, the reader is referred to the web version of this article).

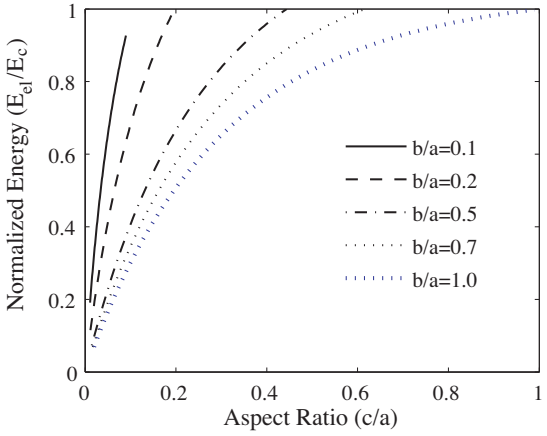

Fig. A1. Elastic energy in the matrix and the transformed region as a function of the aspect ratio of the transformed ellipsoids (semi-axes $a \geq b \geq c$) with a constant volume. Here E_c is the total energy of a spherical particle after the same shear transformation.

nucleation of twinning partials varies from 0.01μ to 0.03μ [58]. The activation volume V^* is another fitting parameter. We will adjust ϕ and the activation volume V^* to fit the softening part of Fig. 1. Rewriting Eq. (8) as

$$\tau = \phi\tau_0 \left[1 - \frac{kT}{\tau_0 V^*} \ln\left(\frac{\beta\pi}{2}\frac{\nu_D}{\dot{\varepsilon}}\frac{d}{\lambda}\sqrt{\frac{\Omega_0}{V^*}}\right)\right] \tag{16}$$

Since the term in $\ln(\cdot)$ changes relatively slower than other terms as V^* changes, we find that the resolved shear stress can be determined by knowing $\phi\tau_0$ and $\tau_0 V^*$; the former is essentially the athermal shear resistance and the latter is the activation energy. A good fit is found in a wide range of τ_0 (from 0.01μ to 0.2μ) as long as we keep $\phi\tau_0 \approx 5.7$ GPa and $\tau_0 V^* = 1.04$ eV. Fig. 6 (solid curve) gives the shear strength of nt-Cu using $\tau_0 = 0.03\mu$ (with $\mu = 45$ GPa), $\phi = 4.2$ and $V^* = 10.6\Omega_0$. The shear strength softening in nano-twinned Cu is well captured using an activation volume of $10.6\Omega_0$. It is found that the predicted shear resistance is very sensitive to the activation volume, which is demonstrated by the other curves with slightly different activation volume while keeping $\tau_0 = 0.03\mu$ and $\phi = 4.2$ unchanged, see Fig. 6 (dotted and dashed lines). Given the values of τ_0 and ϕ trustworthy, the high sensitivity of strength on activation volume enables us to obtain the activation volume. As τ_0 is in the range of 0.01μ to 0.03μ [58], the activation volume changes from $10.6\Omega_0$ to $31.8\Omega_0$, which falls in the region from experiments [35,36,41].

Using Eq. (9), we show the strain-rate sensitivity parameter m vs. twin thickness in Fig. 7. Several different τ_0 are explored while we keep $\phi\tau_0 = 5.7$ GPa and $\tau_0 V^* = 1.04$ eV. The trend of strain-rate sensitivity in nt-Cu – strain-rate sensitivity increases as twin thicknesses decrease – is captured qualitatively. Quantitatively, even in the case that $\tau_0 = 0.001\mu$, the predicted strain-rate sensitivity by Eq. (9) is much higher than the experimental measurement (Fig. 7). This disparity suggests that other mechanisms may also involve with twinning partials mediated de-twinning, which limits the highly rate sensitive process by nucleation controlled plasticity, as explained next.

4.2. The energetic model on twinning/de-twinning

In this case, nucleation is not the bottle-neck for twinning/de-twinning, the energy associated with the twinning/de-twinning process is controlling. From Eq. (13), $\Delta F \leq 0$ favors the transformation by twinning or de-twinning. For Cu, we have $\nu = 0.35$, $\mu = 45$ GPa (at room temperature), $e^T = 0.707$, $\gamma_{tb} = 24$ mJ/m^2 [58], and $\tau_l \approx 10$ MPa [75]. Twins have lengths comparable to grain size d, which is about 500 nm [18]. Fig. 8 gives the model prediction using $\alpha = 0.4$. The softening behavior by de-twinning as λ decreasing from 15 nm is well captured by the model.

For the strength given by Eq. (14) alone, there is no apparent strain rate effect, which is inconsistent with the enhanced strain-rate sensitivity as twin thickness decreases [6,32,35]. Next, we will show the temperature dependence in Eqs. (8) and (14).

4.3. The temperature dependence of strength in nano-twinned Cu

We show in this section the distinct temperature dependences from the kinetics model (Eq. (8)) and the energetic model (Eq. (14)). Fig. 9a gives the yield strength vs. twin thickness for nt-Cu at several temperature, all parameters used here are the same as that for Fig. 8. A slight change in temperature will lead to big difference in strength for nucleation controlled mechanism (black curves in Fig. 9a). The influence of temperature to the energy controlled mechanism is because of the decrease in shear modulus as temperature rises, which is small in a wide range of temperature. For Cu, the shear modulus $\mu_T(T)$ at temperature T (K) is given by [76]

$$\mu_T(T) = \mu\left(1 + \frac{T - 300}{T_M}\right)\frac{T_M}{\mu}\frac{d\mu}{dT}, \quad \frac{T_M}{\mu}\frac{d\mu_T}{dT} = -0.54 \tag{17}$$

where $T_M = 1356$ K for Cu. Fig. 9 shows the temperature dependence of strength ascribed by the kinetic model and the energetic model. While keeping all other parameters unchanged but varying T in Eq. (8) and replacing μ in Eq. (14) by μ_T given above, we obtain the strength vs. twin thickness at several temperature as seen in Fig. 9a. Fig. 9b shows strength vs. temperature curves for nt-Cu samples at several twin thicknesses. The kinetics model predicts a rapid drop in strength as temperature increases but the energy mechanism show negligible strength change as temperature changes. Simple tensile tests [77] and rolling experiments [78] on nt-Cu show very small difference of yield strength (micro-hardness for the latter) at room temperature (300 K) from that at liquid nitrogen temperature (77 K).

5. Conclusion

Starting from the conclusion in [1] that twin partial mediated de-twinning accounts for the strength softening in nt-Cu, we present theoretical models on the strength softening phenomenon in nt-Cu [18] from both kinetic and energetic aspects. The models are then applied to investigate the strain rate and temperature dependences of strengths in nt-Cu. When de-twinning is controlled by the kinetics of twin partial nucleation, the strength of nt-Cu is predicted to $\tau \propto \ln(\lambda/d)$, and the strength is found to be highly strain-rate dependent and temperature dependent; while de-twinning is regarded as a shear transformation mediated by collective motion of twin partials and the free energy change companying with the transformation is controlling, it leads to $\tau \propto \lambda/d$, and the strength is rate independent and weakly depends on temperature. Given the intermediate strain-rate sensitivity and weak temperature dependence on strength in nt-Cu, we suggest that real de-twinning process in nt-Cu may be controlled by both kinetic and energetic mechanisms, which cooperatively determines the strength softening in nt-Cu as twin thickness decreases from 15 nm to 4 nm.

It is interesting to note that the energy controlled mechanism for de-twinning in Eq. (14) is capable to capture several key observations associated with twinning/de-twinning:

(I) shearing directionality of twinning, for example, is represented because shearing strain (e^T in Eq. (14)) by twinning along $<$

$11\bar{2}>$ is only half of that along $<\bar{1}\bar{1}2>$ on (1 1 1) plane [60], and the latter is unlikely to happen;

(II) the "inverse grain-size effect" on twinning [62] can also be explained by Eq. (14): to satisfy $\Delta F<0$, twinning or de-twinning prefers to occur in bigger grains if stresses around grains of different size are more or less the same;

(III) high strain hardening in samples with small λ may result from two effects: (1) the depletion of thin twins that can be easily de-twinned while straining, which results in the increasing of twin thickness in the material and lead to the increasing flow strength, and (2) the tip of de-twinned region involves a dislocation pileup [58], which may harden the materials.

While we use Cu as the model case in this paper because the work is motivated by corresponding experiments [18] and simulations [1] on Cu, the analysis here should be applicable to other nano-twinned f.c.c. metals. Further experimental and computational work are needed to clarify the following interesting issues: (a) temperature dependence of nt-Cu in simple tensile or compressive experiments, especially at elevated temperatures; (b) quantifying the amount of plasticity by de-twinning and that by dislocations inclined to twin planes; (c) Li et al. [1] have shown that that further reducing in grain sizes can achieve even higher strength in nano-twinned f.c.c. metals. Both Eqs. (8) and (14) suggest the same trend. It would be interesting to explore the grain size dependence of the peak strength in nano-twinned metals; (d) identifying the atomic details of dislocation – twin boundary interactions. To mediate de-twinning, twin partials can nucleate from the junctions of twin boundaries and grain boundaries; they could also form via dissociation and/or cross-slip, e.g., dislocations whose Burgers vector is parallel to line of intersection of the twin boundary and the slip plane may cross-slip and glide in the twin boundary [71,79]. Their respective significance in de-twinning is of great interest; and (e) numerically investigating the non-local plasticity governed by nucleation and growth of de-twinning.

Acknowledgements

Y.W. is very thankful to Professor Huajian Gao and Dr. Xiaoyan Li at Brown University for fruitful discussions. Financial support by the "Hundred Talent Program" from the Chinese Academy of Sciences is acknowledged.

Appendix A.

When twinning/de-twinning of a general ellipsoid occurs in a constrained environment, the shape change resulting from the shear deformation of the ellipsoid causes elastic distortion in both the ellipsoid and the surrounding matrix. After transformation, the elastic energy increment in the transformed ellipsoid and the matrix is generally given as [69]

$$E_{el} = 2\gamma\mu(e^T)^2 V \tag{A.1}$$

where γ is a geometrical coefficient relating to the shape of the ellipsoid [69]. It is shown in Fig. A1 that γ is very sensitive to the aspect ratio of c/a in the ellipsoid with semi-axes $a \geq b \geq c$. Two immediate conclusions can be drawn from Fig. A1: (a) the total elastic energy approaches zero as c/a is close to zero; and (b) at a fixed aspect ratio c/a, the energy is minimized if the ellipsoid is an oblate, i.e., $b/a = 1$. This paper deals with an ellipsoid with semi-axes $a = b \gg c$, and Eq. (A.1) is simplified to Eq. (10) in this case [69].

References

[1] X. Li, Y. Wei, L. Lu, K. Lu, H. Gao, Nature 464 (2010) 877–880.
[2] E.O. Hall, Proc. Phys. Soc. Lond. Sect. B 64 (1951) 747–753.
[3] N.J. Petch, J. Iron Steel Inst. 174 (1953) 25–28.
[4] H. Gleiter, Prog. Mater. Sci. 33 (1989) 223–315.
[5] L. Lu, Y. Shen, X. Chen, L. Qian, K. Lu, Science 304 (2004) 422–426.
[6] K. Lu, L. Lu, S. Suresh, Science 324 (2009) 349–352.
[7] K.S. Kumar, S. Suresh, M.F. Chisholm, J.A. Horton, P. Wang, Acta Mater. 51 (2003) 387–405.
[8] D. Wolf, V. Yamakov, S.R. Phillpot, A.K. Mukherjee, H. Gleiter, Acta Mater. 53 (2005) 1–40.
[9] M.A. Meyers, A. Mishra, D.J. Benson, Prog. Mater. Sci. 51 (2006) 427–556.
[10] E. Ma, JOM 58 (2006) 49–53.
[11] M.D. Merz, S.D. Dahlgren, J. Appl. Phys. 46 (1975) 3235–3237.
[12] X. Zhang, A. Misra, H. Wang, T.E. Mitchell, M. Nastasi, J.P. Hirth, J.D. Embury, R.G. Hoagland, Acta Mater. 52 (2004) 995–1002.
[13] X. Zhang, A. Misra, H. Wang, X.H. Chen, L. Lu, K. Lu, R.G. Hoagland, Appl. Phys. Lett. 88 (2006) 173116.
[14] A.M. Hodge, Y.M. Wang, T.W. Barbee Jr., Large-scale production of nano-twinned, ultrafine-grained copper, Mater. Sci. Eng. A 429 (2006) 272–276.
[15] A.M. Hodge, Y.M. Wang, T.W. Barbee Jr., Scripta Mater. 59 (2008) 163–166.
[16] C.J. Shute, B.D. Myers, S. Xie, T.W. Barbee Jr., A.M. Hodge, J.R. Weertman, Scripta Mater. 60 (2009) 1073–1077.
[17] O. Anderoglu, A. Misra, J. Wang, R.G. Hoagland, J.P. Hirth, X. Zhang, Plastic flow stability of nanotwinned Cu foils, Int. J. Plast. 26 (2010) 875–886.
[18] L. Lu, X. Chen, X. Huang, K. Lu, Science 323 (2009) 607–610.
[19] A.H. Chokshi, A. Rosen, J. Karch, H. Gleiter, Scripta Metall. Mater. 23 (1989) 1679–1683.
[20] K. Lu, M.L. Sui, Scripta Metall. Mater. 28 (1993) 1465–1470.
[21] Z. Shan, E.A. Stach, J.M.K. Wiezorek, J.A. Knapp, D.M. Follstaedt, S.X. Mao, Science 305 (2004) 654–657.
[22] S. Yip, Nature 391 (1998) 532–533.
[23] S. Yip, Nature Mater. 3 (2004) 11–12.
[24] J. Schiøtz, F.D. Di Tolla, K.W. Jacobsen, Nature 391 (1998) 561–563.
[25] H. Van Swygenhoven, M. Spaczer, A. Caro, D. Farkas, Phys. Rev. B 60 (1999) 22–25.
[26] J. Schiøtz, K.W. Jacobsen, Science 301 (2003) 1357–1359.
[27] H. Van Swygenhoven, P.M. Derlet, A.G. Froseth, Nat. Mater. 3 (2004) 399–403.
[28] H.H. Fu, D.J. Benson, M.A. Meyers, Acta Mater. 52 (2004) 4413–4425.
[29] Y. Wei, L. Anand, J. Mech. Phys. Solids 52 (2004) 2587–2616.
[30] D.H. Warner, S. Sansoz, J.F. Molinari, Int. J. Plast. 22 (2006) 754–774.
[31] Y.J. Wei, C. Su, L. Anand, Acta Mater. 54 (2006) 3177–3190.
[32] M. Dao, L. Lu, R.J. Asaro, J.T.M. De Hosson, E. Ma, Acta Mater. 55 (2007) 4041–4065.
[33] A. Jerusalem, L. Stainier, R. Radovitzky, Philos Mag. 87 (2007) 2541–2559.
[34] Y.J. Wei, A.F. Bower, H.J. Gao, Acta Mater. 56 (2008) 1741–1752.
[35] L. Lu, R. Schwaiger, Z.W. Shan, M. Dao, K. Lu, S. Suresh, Acta Mater. 53 (2005) 2169–2179.
[36] Y.F. Shen, L. Lu, M. Dao, S. Suresh, Scripta Mater. 55 (2006) 319–322.
[37] L. Xu, D. Xu, K.N. Tu, Y. Cai, N. Wang, P. Dixit, J.H.L. Pang, J. Miao, J. Appl. Phys. 104 (2008) 113717.
[38] Y.B. Wang, M.L. Sui, E. Ma, Philos. Mag. Lett. 87 (2007) 935–942.
[39] T. Kizuka, Japanese J. Appl. Phys. 46 (2007) 7396–7398.
[40] Z.W. Shan, L. Lu, A.M. Minor, E.A. Stach, S.X. Mao, JOM 60 (2008) 71–74.
[41] L. Lu, T. Zhu, Y. Shen, M. Dao, K. Lu, S. Suresh, Acta Mater. 57 (2009) 5165–5173.
[42] A. Frøseth, H. Van Swygenhoven, P.M. Derlet, Acta Mater. 52 (2004) 2259–2268.
[43] Z.H. Jin, P. Gumbsch, E. Ma, K. Albe, K. Lu, H. Hahn, H. Gleiter, Scripta Mater. 54 (2006) 1163–1168.
[44] T. Zhu, J. Li, A. Samanta, H.G. Kim, S. Suresh, Proc. Natl. Acad. Sci. U.S.A. 104 (2007) 3031–3036.
[45] Z.H. Jin, P. Gumbsch, K. Albe, E. Ma, K. Lu, H. Gleiter, H. Hahn, Acta Mater. 56 (2008) 1126–1135.
[46] A.J. Cao, Y.G. Wei, J. Appl. Phys. 102 (2007) 083511.
[47] B. Wu, Y.G. Wei, Acta Mech. Solida Sin. 21 (2008) 189–197.
[48] I. Shabib, R.E. Miller, Acta Mater. 57 (2009) 4364–4373.
[49] C. Deng, F. Sansoz, Nano Lett. 9 (2009) 1517–1522.
[50] L. Li, N.M. Ghoniem, Phys. Rev. B 79 (2009) 075444.
[51] M. Dao, L. Lu, Y.F. Shen, S. Suresh, Acta Mater. 54 (2006) 5421–5432.
[52] A. Jerusalem, M. Dao, S. Suresh, R. Radovitzky, Acta Mater. 56 (2008) 4647–4657.
[53] Y. Kulkarni, R.J. Asaro, Acta Mater. 57 (2009) 4835–4844.
[54] M.S. Daw, M.I. Baskes, Phys. Rev. B 29 (1984) 6443–6452.
[55] S.M. Foiles, M.I. Baskes, M.S. Daw, Phys. Rev. B 33 (1986) 7983–7991.
[56] Y. Mishin, M.J. Mehl, D.A. Papaconstantopoulos, A.F. Voter, J.D. Kress, Phys. Rev. B 63 (2001) 224106.
[57] J. Roth, http://www.itap.physik.uni-stuttgart.de/~imd/index.html.
[58] J.P. Hirth, J. Lothe, Theory of Dislocations, 2nd ed., John Wiley & Sons, Inc., 1982.
[59] E.B. Tadmor, S. Hai, J. Mech. Phys. Solids 51 (2003) 765–793.
[60] M.A. Jaswon, D.B. Dove, Acta Cryst. 9 (1956) 621–626.
[61] S. Kibey, J.B. Liu, D.D. Johnson, H. Sehitoglu, Appl. Phys. Lett. 91 (2007) 181916.
[62] X.L. Wu, Y.T. Zhu, Phys. Rev. Lett. 101 (2008) 025503.
[63] M.F. Meyers, Dynamic Behavior of Materials, John Wiley, New York, 1994, p. 323.
[64] Y.J. Wei, H.J. Gao, Mater. Sci. Eng. A 478 (2008) 16–25.
[65] U.F. Kocks, A.S. Argon, M.F. Ashby, Prog. Mater. Sci. 19 (1975) 1–281.
[66] H. Conrad, in: V.F. Zackey (Ed.), High Strength Materials, 1965.
[67] L. Lu, M. Dao, T. Zhu, J. Li, Script. Mater. 60 (2009) 1062–1066.
[68] A. Kelly, G.W. Groves, Crystallography and Crystal Defects, Longman, London, 1970, p. 290.
[69] J.D. Eshelby, Proc. Roy. Soc. A 243 (1957) 376–396.

[70] J.W. Christian, Acta Metall. 6 (1958) 377–379.
[71] J.W. Christian, S. Mahajan, Prog. Mater. Sci. 39 (1995) 1–159.
[72] T. Waitz, T. Antretter, F.D. Fischer, N.K. Simha, H.P. Karnthaler, J. Mech. Phys. Solids 55 (2007) 419–444.
[73] F. Appel, F.D. Fischer, H. Clemens, Acta Mater. 55 (2007) 4915–4923.
[74] R.J. Asaro, P. Krysl, B. Kad, Philos. Mag. Lett. 83 (2003) 733–743.
[75] L. Xu, D. Xu, K.N. Tu, Y. Cai, N. Wang, P. Dixit, H.L. Pang, J. Miao, J. Appl. Phys. 104 (2008) 113717.
[76] H. Frost, M.F. Ashby, Deformation-Mechanism Maps: The Plasticity and Creep of Metals and Ceramics, Pergamon Press, Oxford, 1982, http://engineering.dartmouth.edu/defmech/.
[77] E. Ma, Y.M. Wang, Q.H. Lu, M.L. Sui, L. Lu, K. Lu, Appl. Phys. Lett. 85 (2004) 4932–4934.
[78] Z.S. You, L. Lu, K. Lu, Script. Mater. 62 (2010) 415–418.
[79] S. Mahajan, Private Communication, 2010.